Whole body distribution of deuterated linoleic and α-linolenic acids and their metabolites in the rat

Yu Hong Lin and Norman Salem, Jr.[1]

Section of Nutritional Neuroscience, Laboratory of Membrane Biochemistry and Biophysics, National Institute on Alcohol Abuse and Alcoholism, National Institutes of Health, Bethesda, MD 20892-9410

Abstract **Little is known about the uptake or metabolism of essential fatty acids (EFAs) in various mammalian organs. Thus, the distribution of deuterated α-linolenic acid (18:3n-3) and linoleic acid (18:2n-6) and their metabolites was studied using a stable isotope tracer technique. Rats were orally administered a single dose of a mixture (20 mg each) of ethyl D5-18:3n-3 and D5-18:2n-6, and 25 tissues per animal were analyzed for D5-labeled PUFAs at 4, 8, 24, 96, 168, 240, 360, and 600 h after dosing. Plasma, stomach, and spleen contained the highest concentrations of labeled precursors at the earliest time points, whereas other internal organs and red blood cells reached their maximal concentrations at 8 h. The time-course data were consistent with liver metabolism of EFAs, but local metabolism in other tissues could not be ruled out. Brain, spinal cord, heart, testis, and eye accumulated docosahexaenoic acid with time, whereas skin accumulated mainly 20:4n-6. On average, ~16–18% of the D5-18:3n-3 and D5-18:2n-6 initial dosage was eventually accumulated in tissues, principally in adipose, skin, and muscle. Approximately 6.0% of D5-18:3n-3 and 2.6% of D5-18:2n-6 were elongated/desaturated and stored, mainly in muscle, adipose, and the carcass. The remaining 78% of both precursors was apparently catabolized or excreted.**—Lin, Y. H., and N. Salem, Jr. **Whole body distribution of deuterated linoleic and α-linolenic acids and their metabolites in the rat.** ***J. Lipid Res.*** **2007.** 48: **2709–2724.**

Supplementary key words docosahexaenoic acid • arachidonic acid • polyunsaturated fatty acid • fatty acid metabolism • stable isotope • gas liquid chromatography-mass spectrometry • essential fatty acid

Although many studies have focused upon the liver as the primary site for essential fatty acid (EFA) metabolism in mammals, relatively little is known about other organs with respect to their uptake of EFA precursors and products or the manner in which these fatty acids are distributed to them. In most human studies, the blood compartment is the only sample available and liver activity must be inferred from plasma analysis, in some cases with the aid of mathematical modeling (1–3). However, efforts to understand and model human EFA metabolism depend upon a rigorous description of EFA metabolism in several organ systems. Although this cannot be achieved in humans for ethical reasons, animal studies allow a complete description of the role of various organs in processing EFAs in vivo. Such a description would include the uptake of the EFA precursors linoleic acid (18:2n-6) and α-linolenic acid (18:3n-3) into various organs as well as their metabolism to various products along the n-3 and n-6 EFA pathways.

Previous investigations include stable isotope studies in primates and have provided analyses of EFA uptake and metabolism of the liver, nervous system, and blood stream (4) and, in some cases, other internal organs such as the heart, lung, and kidney (5). Fu and Sinclair (6, 7) provided a description of the radiolabeling of many guinea pig tissues with [^{14}C]18:2n-6 (6) and [^{14}C]18:3n-3 (7). Whole body balance methods for the analysis of EFA retention in various tissues and β-oxidation (8) as well as those based on breath test using various ^{14}C-labeled EFAs led to the conclusion that the fate of the bulk of the EFAs was β-oxidation (9).

It would be valuable to extend these studies to a description of EFA uptake and metabolism in all of the major tissues in mammals under well-controlled and defined dietary conditions. This information is a first step in the understanding of the EFA requirements and the ability to elaborate and use long-chain polyunsaturates of various organs and tissues throughout the body. The present study was thus designed to investigate the incorporation and metabolism of stable isotope-labeled EFAs into various rat tissues over an extended period. A single oral dose of both $^{2}H_5$-18:3n-3 and $^{2}H_5$-18:2n-6 was given to young adult male rats consuming a defined diet containing 15% of total fatty acids as 18:2n-6 and 3% as 18:3n-3. Negative chemical ionization gas liquid chromatography-mass spectrometry (GC-MS) analysis was used for the quantification of the precursors and their individual metabolites in 25 components from 4 to 600 h after dosing.

Manuscript received 20 August 2007 and in revised form 17 September 2007.

Published, JLR Papers in Press, September 17, 2007.
DOI 10.1194/jlr.M700369-JLR200

Abbreviations: BHT, butylated hydroxytoluene; C_{max}, maximal concentration; D_{max}, maximal amount; EFA, essential fatty acid; GC-MS, gas liquid chromatography-mass spectrometry; GI, gastrointestinal; PFB, pentafluorobenzyl; RBC, red blood cell.

[1] To whom correspondence should be addressed.
e-mail: nsalem@niaaa.nih.gov

MATERIALS AND METHODS

Animals and diet

All animal procedures were carried out in accordance with the National Institutes of Health animal care and welfare guidelines, and the protocol was approved by the National Institute on Alcohol Abuse and Alcoholism Animal Care and Use Committee. Time-pregnant, female Long-Evans hooded rats on the third day of gestation were obtained from Charles River (Portage, MI) at the age of 13 weeks and maintained in our animal facility under conventional conditions with controlled temperature (22°C) and illumination (12 h; 6:00 AM to 6:00 PM); food and water were provided ad libitum. The rats were immediately placed on a pelleted custom diet upon arrival, which was modified from the AIN-93G formulation (10) as described previously (11). In brief, lipid-extracted casein was used, carbohydrate sources were modified, and fat sources (10 wt%) were controlled. Fat sources were 77 g of hydrogenated coconut oil, 18 g of safflower oil, and 5 g of flaxseed oil per kilogram of diet. The fatty acid distribution in the fat was 77% saturated fatty acids, 4% monounsaturated fatty acid, 15% linoleate, 3% α-linolenate, and only traces of longer chain EFAs (C20 and C22). The male offspring were weaned onto the same diet at 3 weeks of age. At 7 weeks of age, nine rats with a body weight of 186 ± 7 g (mean ± SD) were fasted overnight and administrated a single oral dose of 20 mg each of $^2H_5$-18:3n-3 and $^2H_5$-18:2n-6 ethyl ester using olive oil as the vehicle or vehicle oil only for a control animal. The animals were then maintained ad libitum on the above-described diet for the remainder of this "pulse-chase" type of experiment. One animal was euthanized at each of the following time points after dosing with the isotopic tracers: 4, 8, 24, 96, 168, 240, 360, and 600 h. A control animal was euthanized at 0 h. Each rat was dissected into a total of 25 components as detailed below.

Isotope and chemicals

Deuterium-labeled ethyl linolenate ($^2H_5$-17,17,18,18,18-18:3n-3) and deuterium-labeled ethyl linoleate ($^2H_5$-17,17,18,18,18-18:2n-6) were obtained from Cambridge Isotope Laboratories (Andover, MA); isotope purities were >95% for the former and 98% for the latter. No long-chain (>C18) PUFA was found. Chemical purity was >95% as determined by TLC and GC.

Tissue collection

Rats were asphyxiated in carbon dioxide after fasting overnight before euthanasia with the exception of those euthanized at 4 and 8 h, which were given access to food immediately after dosing. Blood was drawn by cardiac puncture when rats were unconscious and separated into plasma and red blood cells (RBCs) at 1,800 *g* for 10 min at 4°C. The head was severed at the neck, and the brain and eye (with associated glands) were removed. The body was placed on ice during this second stage of dissection. Gallbladders were removed before liver and other abdominal tissue collection to avoid contamination with bile fluid. The thymus, salivary, and thyroid glands were dissected out. Abdominal organs collected include the heart, lung, liver, pancreas, kidney, spleen, bladder, and testis. The gastrointestinal (GI) tract (from duodenum to anus) was emptied and rinsed with ice-cold saline (0.85% NaCl); the stomach was subsequently removed and treated similarly. The spinal cord was then separated from the vertebrae. Subsequently, skin with fur was collected from both the skull and carcass, visible subcutaneous fat and visceral fat were pooled, and muscle (skeletal muscle and chest) and bones (short-carpal bones; irregular vertebrae, long humerus, radius, ulna, femur, tibia; flat scapula, ilium) with periosteum and marrow were collected. The brown adipose tissue under the neck skin and along the vertebrae was collected. The remaining carcass contained the skull, ribs, cartilage, paws, tail, and the remaining parts not listed above. After dissection, organs were carefully washed with cold normal saline, blotted, wrapped frozen on dry ice, and then stored in a −80°C freezer until analysis. Each of the 25 components listed in **Table 1** were analyzed individually. In some cases, for graphic purposes, individual tissues were combined to make 11 categories (adipose, skeleton, circulatory system, digestive system, muscle, nervous system, respiratory system, skin, urogenital system, and the remaining carcass), as detailed in **Fig. 1**. Excretions were not collected.

Homogenization, lipid extraction of various tissues, and derivatization reactions

Large organs/tissues were thoroughly diced into fine pieces at 4°C before extraction. Organs were homogenized in methanol containing 0.2 mM butylated hydroxytoluene (BHT; 10 ml for 1 g of tissue); one aliquot of homogenate (~100 mg of tissue wet weight) was used for total lipid extraction. A motor-powered small tissue homogenizer was used for tissue disruption (Omni International, Marietta, GA). Bones were cut into smaller pieces, cooled with liquid nitrogen, and pulverized into a fine powder with a mortar and pestle over dry ice. One gram of this bone powder was placed in 10 ml of methanol-BHT and sonicated for 10 min (12). The skin/fur was cut to separate the skin from fur and the subcutaneous fat, which was combined with the white adipose tissue. Skin samples of ~1 cm^2, containing both epidermis and dermis, were taken from various parts of the rat body and diced into <3 mm^2 pieces, mixed completely, and then homogenized (10 ml of methanol-BHT for 1 g of skin sample). One gram of fur from various areas was cut into lengths of <3 mm over dry ice and sonicated in 10 ml of methanol-BHT for 20 min. The carcass was handled similarly to bone: after freezing on dry ice and powdering with a mortar and pestle, 5 g of carcass powder was sonicated in 50 ml of methanol-BHT. White adipose tissue from different body locations was diced and mixed well, and ~0.25 g of adipose was homogenized in 5 ml of chloroform-methanol (2:1)-BHT solution.

One aliquot of homogenate or sonicate from each tissue was used to extract total lipids of the tissues according to Folch, Lees, and Sloane-Stanley (13). The total lipid extract was dried under a stream of nitrogen and transmethylated using boron trifluoride in methanol (14 g/l; Sigma Chemical, St. Louis, MO) as described by Morrison and Smith (14) and modified by Salem, Reyzer, and Karanian (15). The internal standard, 22:3n-3 ethyl ester (60 nmol/sample), was added to each sample before lipid extraction. A separate aliquot of the homogenate was hydrolyzed and derivatized with pentafluorobenzyl (PFB) reagent [PFB bromide, diisopropylamine in acetonitrile (1:100:1,000, v/v/v)] to form fatty acid PFB ester for GC-MS negative chemical ionization analysis (16) for deuterium-labeled fatty acids. For GC-MS analysis, 2.5 nmol/sample of 22:3n-3 ethyl ester was added at the beginning of the lipid extraction as an internal standard.

GC-MS analysis

An Agilent 5973 mass spectrometer equipped with an Agilent 6890 GC Plus LAN system (Agilent Technologies, Inc., Wilmington, DE) was used for the quantification of deuterated fatty acids. An aliquot of 1 μl of fatty acid PFB ester per sample was injected onto a DB-FFAP (free fatty acid phase) capillary column (15) interfaced directly into the negative chemical ionization system using methane as the reagent gas. The GC oven temperature was programmed from 125°C to 245°C at 8°C followed by holding for 37 min. Selected ion monitoring of the base peak (M-PFB) for the analytes of interest, both the precursors and the main metabolites, was carried out with continuous monitoring and

TABLE 1. D_{max} of deuterated 18:3n-3, 22:6n-3, 18:2n-6, and 20:4n-6 in 25 rat tissues

No.	Tissues	Tissue Weight (g, at 240 h)	$^2H_5$-18:3n-3		$^2H_5$-22:6n-3		$^2H_5$-18:2n-6		$^2H_5$-20:4n-6	
			D_{max}	T_{max}	D_{max}	T_{max}	D_{max}	T_{max}	D_{max}	T_{max}
1	Adipose, brown	0.5	0.26	24	0.02	168	0.25	24	0.004	168
2	Adipose, white	28.9	**14.5**	168	**0.80**	360	**15.7**	168	**0.16**	168
3	Adrenal gland[a]	0.1	0.004	4	0.004	96	0.01	8	0.01	96
4	Bladder	0.1	0.003	8	0.002	240	0.004	8	0.004	240
5	Bone	12.2	0.25	8	0.21	240	0.25	8	0.10	240
6	Brain	1.9	Tr		0.10	600	0.01	8	0.02	240
7	Carcass	48.3	**0.84**	8	**0.99**	240	**1.04**	8	**0.44**	240
8	Eye	0.6	0.005	168	0.01	240	0.01	24	0.004	240
9	Fur	2.3	0.20	4	0.004	96	0.12	4	0.004	96
10	Heart	1.0	0.04	8	0.08	168	0.09	8	0.03	240
11	Intestine[b]	3.0	0.59	4	0.06	168	0.68	8	0.08	168
12	Kidney	2.1	0.12	8	0.07	96	0.18	8	0.08	168
13	Liver	11.1	**4.48**	8	**1.69**	96	**4.35**	8	**0.78**	96
14	Lung	1.1	0.03	8	0.03	96	0.08	8	0.03	168
15	Muscle	67.7	**2.14**	8	**2.56**	600	**3.72**	8	**0.69**	360
16	Plasma	6.5	0.19	4	0.08	96	0.40	8	0.06	96
17	Pancreas	0.4	0.01	8	0.02	240	0.04	8	0.03	240
18	Red blood cell	5.3	0.01	8	0.01	96	0.06	8	0.02	240
19	Skin	31.0	**3.82**	96	**0.31**	168	**2.88**	96	**0.38**	168
20	Salivary gland	0.2	0.01	8	0.01	240	0.01	8	0.01	240
21	Spinal cord	0.5	ND		0.03	600	0.003	8	0.003	600
22	Spleen	0.9	0.01	4	0.01	96	0.03	8	0.02	96
23	Stomach	1.2	0.19	4	0.01	168	0.20	8	0.03	168
24	Thymus gland	0.5	0.004	8	0.003	96	0.02	24	0.01	168
25	Testis	2.6	0.004	8	0.03	168	0.04	24	0.03	240

D_{max}, maximal amount, expressed as percentage of the dose at T_{max}; ND, nondetectable; T_{max}, time corresponding to the greatest tissue content; Tr, trace values (i.e., <0.002). Boldface numbers indicate the five greatest values for the 25 tissues examined.

[a] Adrenal gland included thyroid gland and mandibular lymph nodes.

[b] Intestine included duodenum, small intestines, and cecum.

quantitated according to a previously reported method (17). For the measurement of unlabeled fatty acid concentrations in tissues for the calculation of enrichment, GC-flame ionization detection analysis was performed on an Agilent 6890 Plus LAN system as described previously (15).

Data analysis

Isotopically labeled EFA data were expressed as the concentration, in nanomoles per gram of tissue wet weight or, for plasma and RBCs, as nanomoles per milliliter. Because animals were euthanized over a period of 25 d while still being fed nonlabeled food and growing, initial body weight and tissue weight were lower than at the end of the experiment (Fig. 1, bottom). Thus, the fatty acid concentration values were normalized to the body weight by multiplying the concentration values by the ratio of the tissue weight at each time point to the initial (time = 0) tissue weight. The amount of each labeled fatty acid per tissue was obtained by multiplying the concentration by the weight of the whole tissue. The distribution of each labeled fatty acid in the rat whole body was computed as a percentage by dividing the amount of the labeled fatty acid in a particular tissue by the sum of the labeled fatty acid in all of the organs/tissues × 100 at each time point. Areas under the curves were obtained by integrating the areas under the curves as a function of time using a trapezoid estimation method (18).

RESULTS

Tissue dissection

Animals were dissected into 25 components, which may be subgrouped into 11 biological systems (Fig. 1). The proportion of total rat body weight that was recovered in harvested tissues at the various time points was 82 ± 5% (n = 9). Of this total collected tissue, the largest components were muscle (29 ± 2%), skin (16 ± 1%), adipose (13 ± 3%), bone (4.7 ± 0.8%), and liver (4.6 ± 0.4%); the remaining carcass amounted to 20 ± 1%. The weight of the circulatory system, nervous system, respiratory system, urogenital system, and remaining digestive system constituted the remaining ~12% of total tissue wet weight (Fig. 1). During the 4 week duration of the experiment, body weight increased by ~2-fold from 194 to 383 g. During this period, there was an increased percentage of tissue as adipose, but the proportion of various organs and tissues in the various biological systems was relatively constant. The tissue distribution of precursors and their main intermediates as well as the metabolic end products was identified and determined in all 25 components harvested, as presented below.

Time course of deuterated n-3 EFA concentrations in principal organs

The appearance and disappearance of $^2H_5$-18:3n-3 in various tissues and its major in vivo metabolites are presented in **Fig. 2** as bar graphs at various time points after a single oral dose of $^2H_5$-18:3n-3. The precursor was at its maximal concentration (C_{max}; in nmol/g or nmol/ml) at the first experimental time point of 4 h in the stomach (112), plasma (15.6), and spleen (12.4) and decreased sharply by 8 h. However, several other tissues also achieved C_{max} precursor concentrations at ~8 h, including RBCs

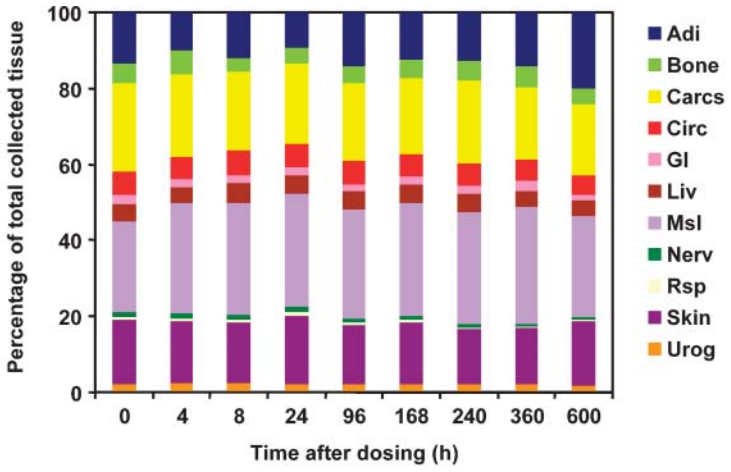

Dissection Category	Abbr.	Tissues Harvested	Percent of Harvested Tissue
Adipose tissue	**Adi**	Brown, white adipose	13.2 ± 3.2
Skeleton	**Bone**	Skeletal bones, spine	4.7 ± 0.8
Carcass	**Carcs**	Any tissue not listed in other categories	20.4 ± 1.5
Circulatory system	**Circ**	Heart, plasma, RBC, spleen	5.9 ± 0.5
Digestive system	**GI**	Gastrointestinal tract: including pancreas, stomach, duodenum, small intestines, cecum	2.0 ± 0.3
	Liv	Liver	4.6 ± 0.4
Muscle	**Msl**	Skeletal muscle	29.2 ± 2.2
Nervous system	**Nerv**	Brain, spinal cord	1.2 ± 0.3
Respiratory system	**Rsp**	Lung	0.6 ± 0.1
Skin	**Skin**	Skin, fur	16.1 ± 1.2
Urogenital system	**Urog**	Kidney, urinary bladder, testis	2.1 ± 0.2

Time point (h)	0	4	8	24	96	168	240	360	600
Body weight (g)	194	198	182	183	223	249	280	321	383

Fig. 1. Rats were dissected into 25 components (see Table 1) and then organized into 11 categories, as depicted in the lower panel. The percentage of the total collected tissue is given for each of these 11 organ systems at each time point between 0 and 600 h in the top panel. The mean values ± SD are given for nine rats from 7 to 11 weeks old in the bottom panel. The body weight of each rat at the time of euthanasia is also given at the bottom of the figure. RBC, red blood cell.

(2.6), liver (403), heart (27.8), kidney (47.3), lung (20.2), and testis (1.7). In the eye, $^2H_5$-18:3n-3 showed values near 3–4 over much of its time course, with a maximum at 168 h (6.8). Very little precursor was detected in brain and spinal cord.

A somewhat different pattern was observed for the metabolites derived from $^2H_5$-18:3n-3 in vivo. As the principal location of fatty acid metabolism, the liver showed the highest concentration of $^2H_5$-20:5n-3 (17.7), $^2H_5$-22:5n-3 (42.5), and $^2H_5$-22:6n-3 (152) compared with other organs. $^2H_5$-20:5n-3 was detected in liver at 4 h, reached a maximum at 8 h, maintained a high level after 24 h, and decreased more slowly than its precursor, $^2H_5$-18:3n-3. A similar pattern was seen for 20:5n-3 in spleen (2.1), brain (0.2), spinal cord (0.6), kidney (5.1), and testis (2.6). RBCs (1.0), stomach (2.8), heart (1.8), lung (5.9), and eye (0.4) showed a slower appearance and disappearance of $^2H_5$-20:5n-3. For $^2H_5$-22:5n-3, C_{max} was observed at 24–96 h after dosing in nearly all tissues. The liver $^2H_5$-22:5n-3 peaked at 24 h and had a rather rapid disappearance afterward. Brain and spinal cord were somewhat unusual in that the decay of $^2H_5$-22:5n-3 was slow after the 96 h peak.

$^2H_5$-22:6n-3 showed a much different appearance and disappearance pattern in various organs relative to its precursor. Liver showed a maximal concentration at 96 h, along with plasma, lung, spleen, and kidney, and then decreased gradually. $^2H_5$-22:6n-3 was still detectable at 600 h in blood and the main organs. However, $^2H_5$-22:6n-3 appeared in brain, spinal cord, testis, and eye by 4–8 h, reached a maximal or near maximal concentration by 96 h, and thereafter maintained a high level until the end of the experimental period at 600 h. The brain and spinal cord appeared to be continuously accreting $^2H_5$-22:6n-3 over the entire course of the experiment, as its concentration was still increasing at the last time point at 600 h. The concentrations of the precursors ($^2H_5$-18:3n-3, $^2H_5$-20:5n-3, and $^2H_5$-22:5n-3) in the nervous system were much lower than that of $^2H_5$-22:6n-3.

Whole body distribution of $^2H_5$-18:3n-3 content

The total amount of $^2H_5$-18:3n-3 per organ was computed from the concentration data, and the tissue totals were added to calculate the whole body total. The data for each tissue system were then expressed as a percentage of the whole body total $^2H_5$-18:3n-3 at each time point (**Fig. 3A**). At 4 h, a large amount of the $^2H_5$-18:3n-3 was observed in the GI tract (15%), muscle (20%), and liver (27%). By 8 h, the GI amount was rapidly decreasing, although still present (6%), liver had increased significantly to 39% of total, and muscle (19%) and adipose (16%) contained significant proportions of the whole body $^2H_5$-18:3n-3. By 24 h, GI tract $^2H_5$-18:3n-3 was essentially gone, liver content had decreased (19%), and muscle (27%) and skin (14%) percentages had increased; adipose $^2H_5$-18:3n-3 has increased dramatically to 34% of total. By 96 h, liver $^2H_5$-18:3n-3 was nearly gone, with adipose containing the bulk (71%) and substantial amounts also in the skin (20%). Later

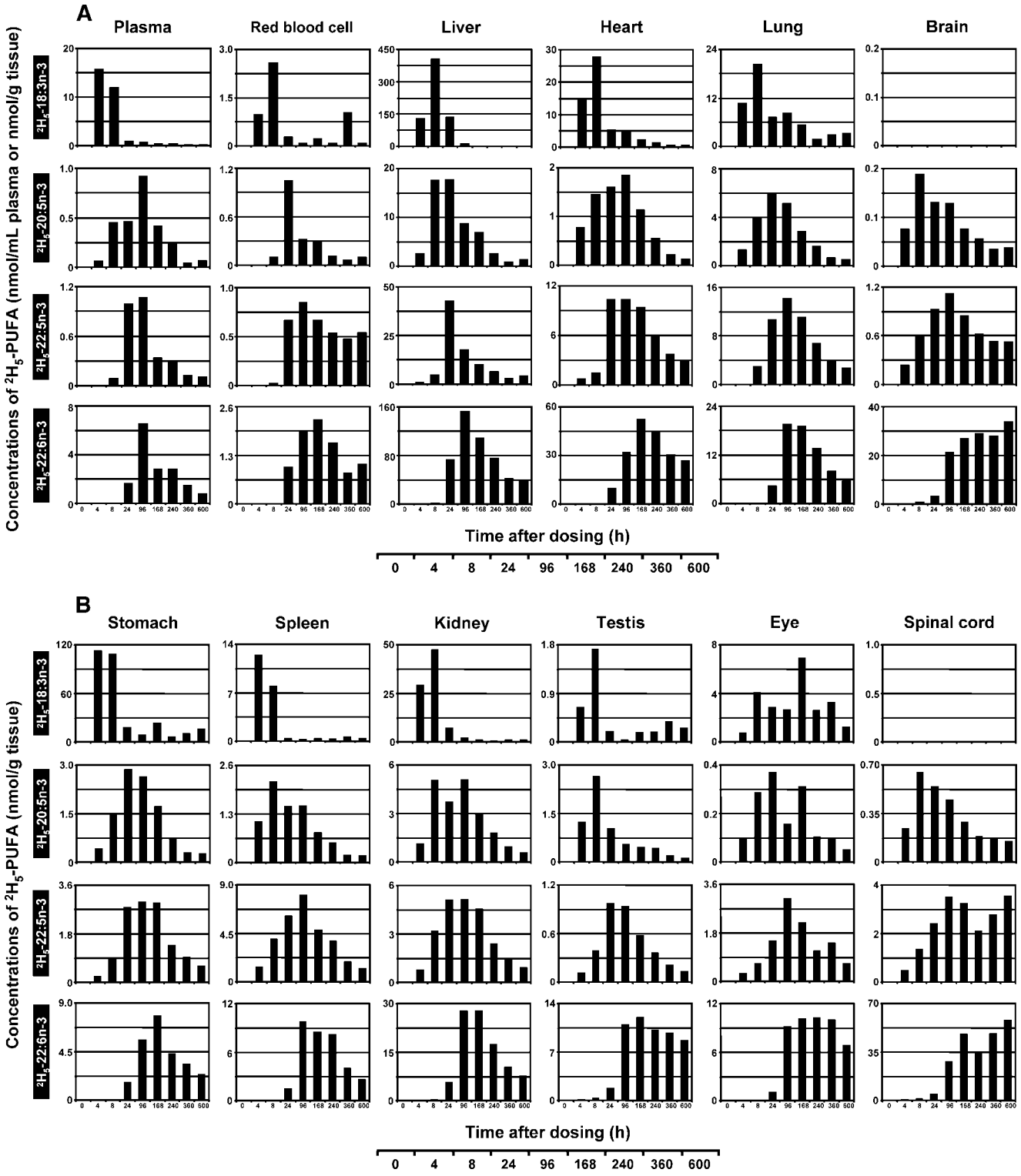

Fig. 2. Time-course plots of the concentrations (nmol/g wet tissue and nmol/ml for plasma and RBCs, respectively) of $^2H_5$-18:3n-3 and its main in vivo metabolites $^2H_5$-20:5n-3, $^2H_5$-22:5n-3, and $^2H_5$-22:6n-3 in rat plasma, RBCs, liver, heart, lung, and brain (A) and in stomach, spleen, kidney, testis, eye, and spinal cord (B) as a function of time over 600 h after a single oral dosing. Values were derived from one animal at each time point.

time points were similar to the 96 h time point in that the major reservoirs for $^2H_5$-18:3n-3 were primarily adipose and, to a lesser extent, skin and muscle. Very little $^2H_5$-18:3n-3 was detected in the nervous system.

An estimate of the amount of $^2H_5$-18:3n-3 recovered in the whole body was made by adding the amounts found in the individual compartments (Fig. 3B). After the initial period, in which it was noted that some $^2H_5$-18:3n-3 label

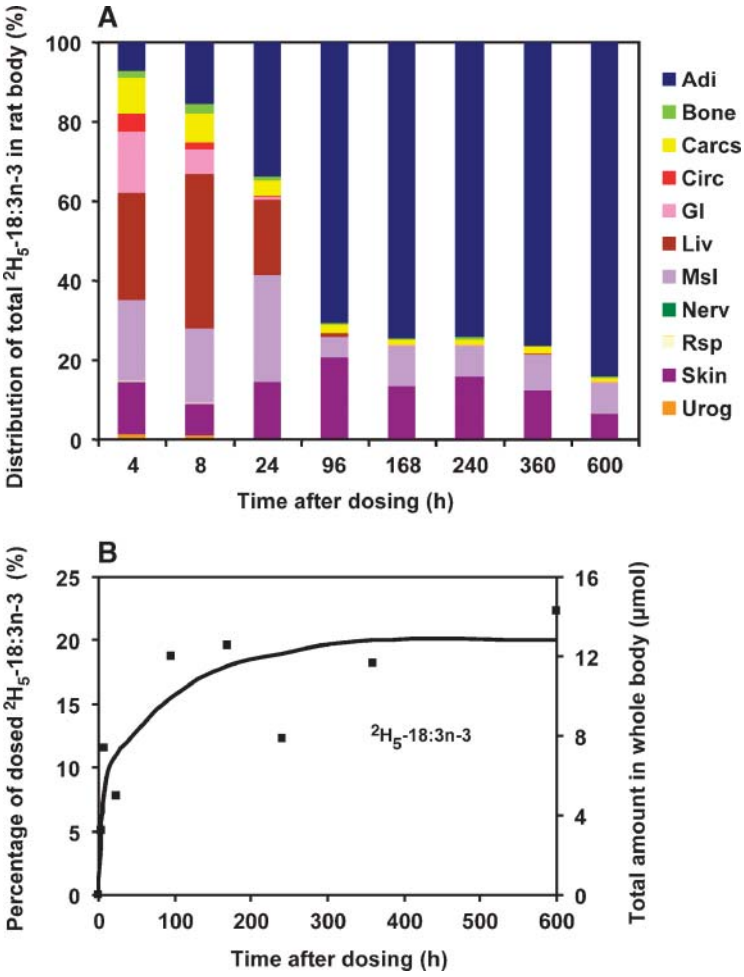

Fig. 3. Distribution of $^2H_5$-18:3n-3 deposited in various rat organ systems versus time. The data are expressed as a percentage of the total recovered $^2H_5$-18:3n-3 at each time point in A. The total amount and the percentage of the initial dose for $^2H_5$-18:3n-3 are presented in B. Values were derived from one animal at each time point. The abbreviations for each organ system are as in Fig. 1.

was lost as a result of rinsing of the GI system after dissection, a plateau was reached by 96 h and maintained until the end of the experiment at 600 h at a level of ~20% of the initial dose.

Whole body distribution of $^2H_5$-18:3n-3 metabolites

Total $^2H_5$-18:3n-3 metabolites per each tissue, including $^2H_5$-20:3n-3, $^2H_5$-20:4n-3, $^2H_5$-20:5n-3, $^2H_5$-22:5n-3, and $^2H_5$-22:6n-3, were calculated at each time point and are displayed in **Fig. 4**. The contents of each of these metabolites were summed at each time point and for each tissue to make a total value, and then the percentage of the total was plotted for each of the main organ systems. Initially, at 4 h, in addition to the high liver content (14%), carcass (21%), muscle (17%), and skin (18%) also contained substantial percentages of the whole body n-3 metabolites. The GI system reached its peak level of n-3 metabolites, composed primarily of $^2H_5$-20:5n-3, at 4 h, and this diminished during the next several days. The liver content was substantial, reaching its peak (50%) after 24 h; thereafter, it decreased to 30% at 96 h and then continued to decrease gradually during the remainder of the 600 h experiment. Muscle was labeled rapidly with n-3 metabolites, with a substantial percentage on the first day, and thereafter continued to accrete, becoming the predominant tissue after 168 h; the n-3 metabolite here was primarily $^2H_5$-22:6n-3. Adipose content of n-3 metabolites was initially 8%, increasing gradually afterward until ~168 h (16%), after which it remained almost constant. Skin labeling was interesting in that it reached its maximum metabolite value of 18% at the initial time point of 4 h and then diminished afterward to 4% by 600 h. The circulatory system maintained a consistent percentage of ~1–3% during the entire experimental period. The nervous system increased gradually and reached ~2% at the end of study, although accounting for only 1% of the total tissue weight. Initially, the n-3 fatty acid metabolites were composed mainly of $^2H_5$-20:5n-3, with $^2H_5$-22:5n-3 being produced soon after. By 240–600 h, $^2H_5$-22:6n-3 became the principal n-3 metabolite.

Concentration time-course plots of deuterated n-6 EFA in principal organs

The appearance and disappearance of $^2H_5$-18:2n-6 and its in vivo metabolites in various organs are presented in **Fig. 5A, B** as bar plots of isotope concentration versus time after a single oral dose of $^2H_5$-18:2n-6.

The $^2H_5$-18:2n-6 precursor exhibited a maximal concentration at 8 h for plasma, RBCs, and all organs except testis and eye, in which $^2H_5$-18:2n-6 was taken up more slowly and reached a peak after 24 h. As might be expected, the stomach isotope content reached its greatest concentration at the earliest time points used, reaching 105–120 nmol/g

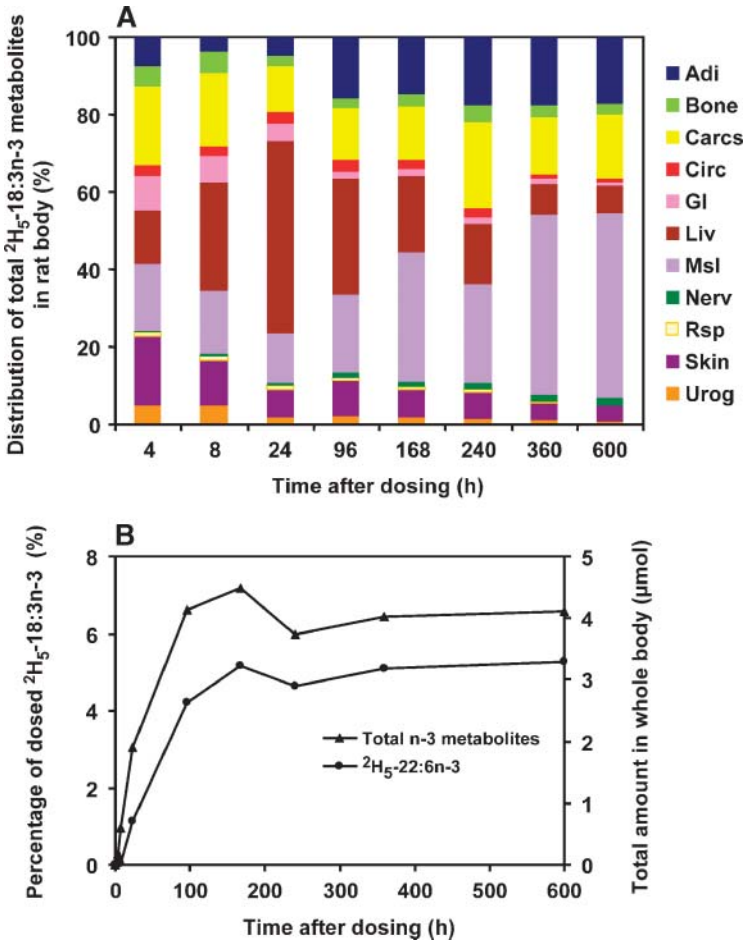

Fig. 4. Distribution of n-3 metabolites, including $^2H_5$-20:3n-3, $^2H_5$-20:4n-3, $^2H_5$-20:5n-3, $^2H_5$-22:5n-3, and $^2H_5$-22:6n-3, synthesized from $^2H_5$-18:3n-3 in rat organ systems versus time. The data are expressed as a percentage of the total recovered n-3 deuterated metabolites at each time point in A. The total amount of n-3 metabolites and $^2H_5$-22:6n-3 derived from $^2H_5$-18:3n-3 and the percentage of the initial $^2H_5$-18:3n-3 dose are presented in B. Values were derived from one animal at each time point. The abbreviations for each organ system are as in Fig. 1.

tissue weight at 4–8 h. The pattern of precursor uptake for plasma, spleen, and heart resembled the uptake of $^2H_5$-18:2n-6 in stomach, with a high 4 h value and peaking at 8 h. After reaching its maximal value, $^2H_5$-18:2n-6 disappearance from the plasma, RBCs, liver, stomach, and spleen was rapid. Brain and spinal cord did become rapidly labeled with the $^2H_5$-18:2n-6, although the concentrations were relatively low. A high concentration of $^2H_5$-18:2n-6 was reached in the liver, stomach, kidney, heart, and lung.

As expected in a metabolic sequence of reactions, each metabolite of $^2H_5$-18:2n-6 generally appeared in each tissue, with a slight delay with respect to its precursor. An exception was $^2H_5$-22:5n-6, which generally reached its maximum at about the same time as the $^2H_5$-22:4n-6 maximum within the resolution of this experiment. The plasma and liver exhibited essentially the same maxima for each successive $^2H_5$-18:2n-6 metabolite, indicating a rapid equilibration of these compartments. As the principal location of fatty acid metabolism, liver exhibited the greatest concentrations of $^2H_5$-18:3n-6, $^2H_5$-20:3n-6, and $^2H_5$-20:4n-6 compared with other organs. However, for $^2H_5$-22:4n-6 and $^2H_5$-22:5n-6, testis showed 2- and 6-fold greater maximal concentrations, respectively, than did liver. For $^2H_5$-18:3n-6, heart and lung showed much slower elimination, and nervous system along with the eye showed no detectable uptake. For $^2H_5$-20:3n-6, a slow decay was observed in most organs, particularly in the nervous system. Most of the internal organs exhibited a somewhat delayed pattern of metabolism compared with the liver/plasma, especially for the formation of $^2H_5$-20:4n-6 and its metabolites. Liver showed a maximal concentration of $^2H_5$-20:4n-6 at 96 h, decreased gradually, and then reached a plateau. In contrast, the brain, spinal cord, eye, testis, RBCs, and heart tended to remain near or at the maximal $^2H_5$-20:4n-6 concentration for an extended period. Deuterated 22:4n-6 also exhibited an extended plateau pattern for RBCs, stomach, spinal cord, kidney, testis, eye, liver, and brain. $^2H_5$-22:5n-6 accumulated in several tissues with time, including the heart, brain, spinal cord, testis, RBCs, and eye.

Whole body distribution of $^2H_5$-18:2n-6

The whole body distribution of the $^2H_5$-18:2n-6 precursor at different times after dosing is presented in **Fig. 6A**. Again, the total amount of $^2H_5$-18:2n-6 per organ was computed from the concentration data, and the organ totals were added to calculate the whole body total. The data for each organ system were then expressed as a percentage of the whole body total $^2H_5$-18:2n-6 at each time point. At 4 h after administration, ~16% of the $^2H_5$-18:2n-6 appeared in the GI tract, with 12% in liver, whereas muscle was the principal depot, as it accumulated 31% of the whole body total. Approximately 10% each appeared in skin and adi-

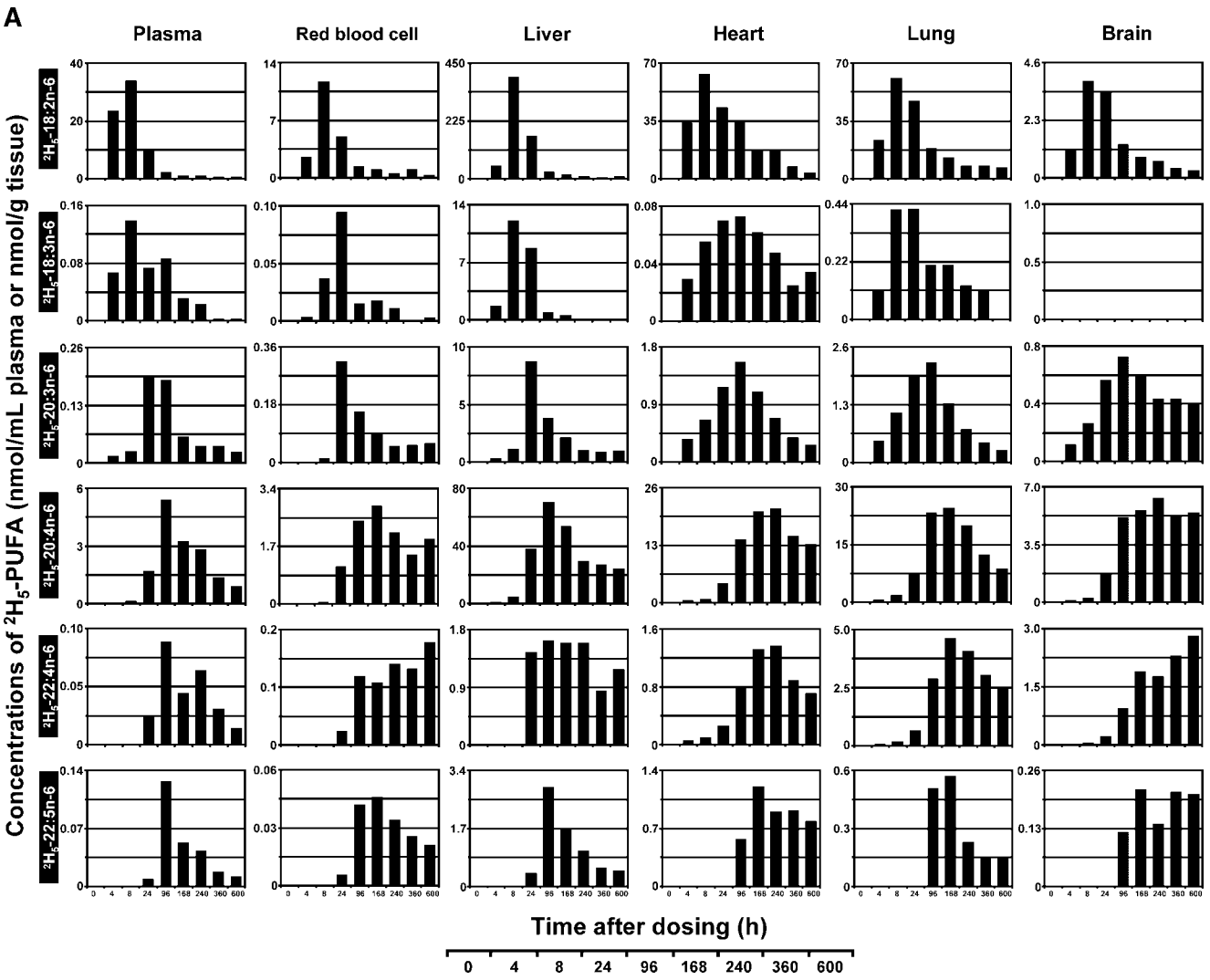

Fig. 5. Time-course plots of the concentrations (nmol/g wet tissue and nmol/ml for plasma and RBCs, respectively) of $^2H_5$-18:2n-6 and its principal in vivo metabolites $^2H_5$-18:3n-6, $^2H_5$-20:3n-6, $^2H_5$-20:4n-6, $^2H_5$-22:4n-6, and $^2H_5$-22:5n-6 in rat plasma, RBCs, liver, heart, lung, and brain (A) and in stomach, spleen, kidney, testis, eye, and spinal cord (B) as a function of time over 25 days after a single oral dosing. Values were derived from one animal at each time point.

pose tissue. The circulation system accounted for ~8% at 4 h; this decreased after 8 h and nearly disappeared by 96 h. $^2H_5$-18:2n-6 increased in liver after 4 h, reached a maximum at 8 h, and then decreased sharply after 24 h. Muscle accounted for 27% at 8 h, decreased gradually, and then was relatively constant at ~10% between 96 and 600 h. White adipose tissue markedly increased $^2H_5$-18:2n-6 after 8 h and became the predominant depot at 4 d (75%) and afterward. Skin also played a significant role in accumulating $^2H_5$-18:2n-6, with a consistent level of ~10% (range, 7–14%) after the 8 h time point. Distinct from the behavior with $^2H_5$-18:3n-3, the nervous system accumulated a small amount of $^2H_5$-18:2n-6. In summary, 96 h after a single dose of $^2H_5$-18:2n-6, the unmodified acid was found mainly in adipose tissue and secondarily in muscle and skin.

An estimate of the amount recovered in the whole body was made by adding the amounts of $^2H_5$-18:2n-6 found in the individual compartments (Fig. 6B). After the initial period, when some of the $^2H_5$-18:2n-6 label was lost as a result of rinsing of the GI system after dissection, a plateau was reached by 96 h and maintained until the end of the experiment at 600 h at a level of ~20% of the initial dose, similar to the findings for $^2H_5$-18:3n-3.

Whole body distribution of $^2H_5$-18:2n-6 metabolites

The sum of the $^2H_5$-18:2n-6 metabolites $^2H_5$-18:3n-6, $^2H_5$-20:3n-6, $^2H_5$-20:4n-6, $^2H_5$-22:4n-6, and $^2H_5$-22:5n-6 in liver began at a high level (33%) at 4 h and reached a maximum (48%) at 24 h, with a subsequent slow decay over the course of this study (**Fig. 7A**). The n-6 metabolite that decreased in the liver after 96 h appeared to be transferred mainly to muscle, with a smaller increment in adipose. The circulatory system maintained a percentage of 2–5% during the entire experimental period. n-6 metabolites in the GI tract peaked at 4 h, in conformity with the early peak in $^2H_5$-18:2n-6, and then decreased throughout the 600 h time course of the

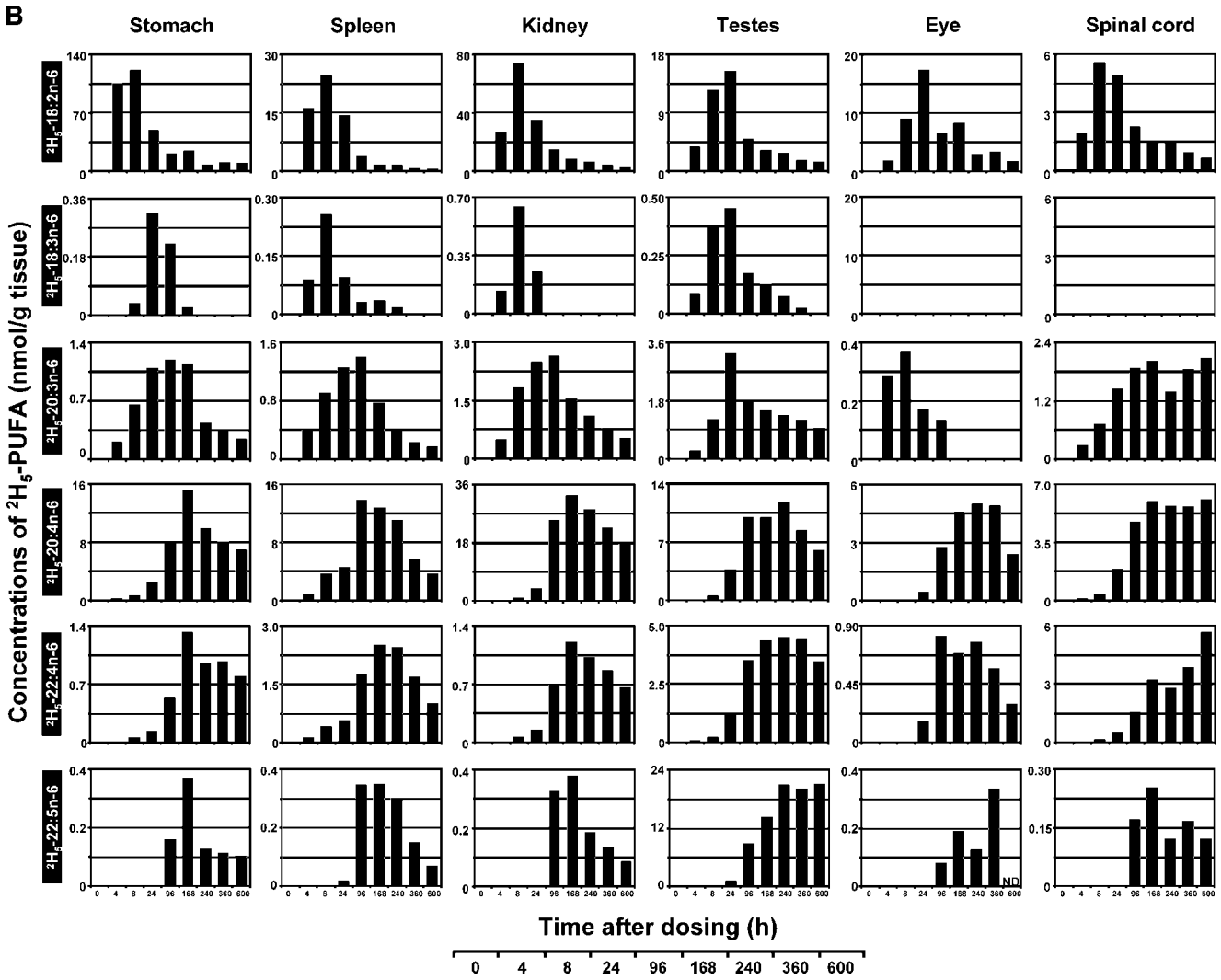

Fig. 5.—*Continued.*

experiment to 1.5% of the whole body total. Similar to the case for the n-3 metabolites, muscle played an important role in the tissue distribution of n-6 metabolites, with ~8–15% in the first days and increasing to ~35% by 360–600 h. N-6 metabolites in skin were initially very low at 4 h but thereafter increased to a level of ~14–15% from 96 to 240 h. The nervous system eventually accumulated ~1% of total body n-6 metabolites, mainly in the form of $^2H_5$-20:4n-6. The urogenital system accumulated ~3.2% by 24 h, increasing to 5.1% by 600 h mainly as a result of the accretion of $^2H_5$-22:4n-6 and $^2H_5$-22:5n-6 in the testis as well as $^2H_5$-20:4n-6 in kidney. $^2H_5$-20:4n-6 was the major metabolite of $^2H_5$-18:2n-6 found in the whole body throughout the time course (Fig. 7B).

Maximal total amount of precursors and principal metabolites in various organs

The total amount of the various deuterated fatty acids in each organ at the time point at which it reaches its maximal value (D_{max}) was calculated. Thus, this calculation was made for $^2H_5$-18:3n-3, $^2H_5$-22:6n-3, $^2H_5$-18:2n-6, and $^2H_5$-20:4n-6 and then expressed as the percentage of total precursor dose (Table 1). White adipose tissue became the main repository for the two precursors, accounting for 14.5% of the dose for $^2H_5$-18:3n-3 and 16% of the dose for $^2H_5$-18:2n-6, although this content was not reached until 168 h after dosing. The white adipose had much greater precursor content than did the brown adipose, likely because of its greater tissue weight. Liver was a somewhat distant second with respect to content of unmodified EFA precursor, with 4.5% of the $^2H_5$-18:3n-3 dose and 4.4% of the $^2H_5$-18:2n-6 dose at the 8 h time point. Skin and muscle also contained a substantial percentage of precursor dose, as both isotopes were in the 2–4% range. For both $^2H_5$-22:6n-3 and $^2H_5$-20:4n-6, liver and muscle were the two major compartments, with liver content peaking (1.7% and 0.8% of dose for $^2H_5$-22:6n-3 and $^2H_5$-20:4n-6, respectively) after 96 h, whereas muscle content (2.6% and 0.7% of dose for $^2H_5$-22:6n-3 and $^2H_5$-20:4n-6, respectively) was greatest after 360–600 h. The principal metabolites in skin and adipose exhibited maxima in the 168–360 h range. The carcass also contained a considerable amount of both precursors

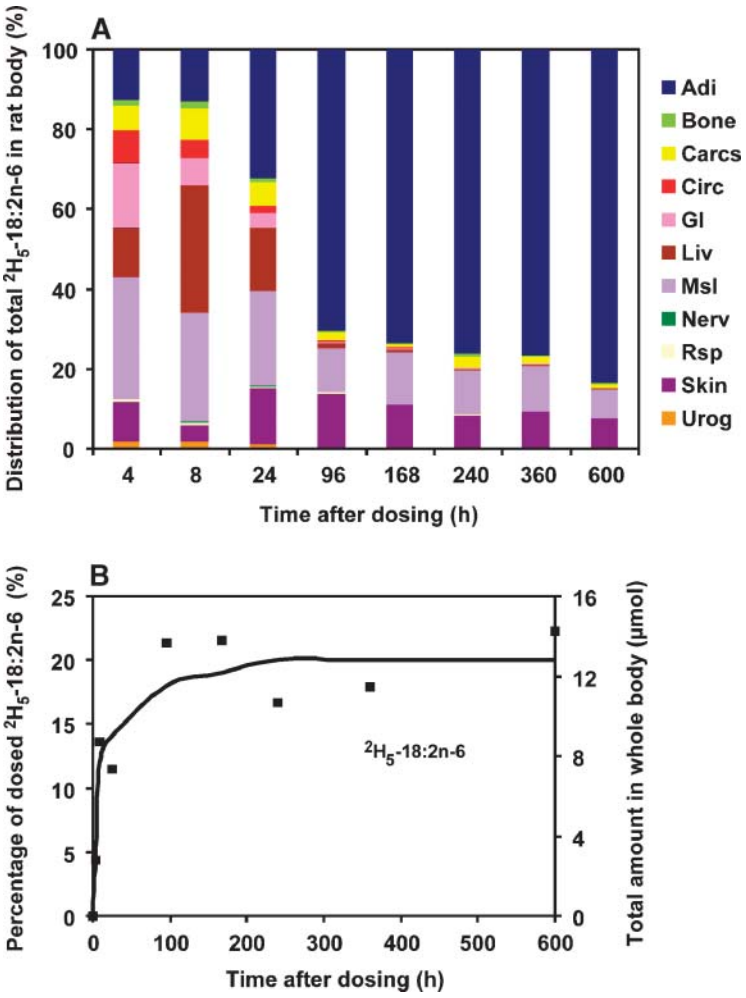

Fig. 6. Distribution of $^2H_5$-18:2n-6 deposited in various rat organ systems versus time. The data are expressed as a percentage of the total recovered $^2H_5$-18:2n-6 at each time point in A. The total amount and the percentage of the initial dose for $^2H_5$-18:2n-6 are presented in B. Values were derived from one animal at each time point. The abbreviations for each organ system are as in Fig. 1.

and major metabolites, perhaps because of small muscles (including the diaphragm and rib muscles) and bits of adipose that could not be readily dissected out. The digestive system did not exhibit a very substantial percentage of the dose at any time point, likely because of the absence of sampling at very short time points (<4 h). It is noteworthy that the distribution (defined in Data Analysis above) of the precursors $^2H_5$-18:2n-6 and $^2H_5$-18:3n-3 is quite similar throughout the body. The values of their metabolites are also somewhat similar, although the values for $^2H_5$-22:6n-3 were generally higher than those for $^2H_5$-20:4n-6.

To quantify all 25 tissues with respect to the plot of the total amount per organ at each time point, the area under the curves was calculated (**Table 2**). For the precursors $^2H_5$-18:3n-3 and $^2H_5$-18:2n-6, expressed as micromoles per hour, white adipose tissue accumulated the most (5,082 and 5,435, respectively), followed by skin (845 and 701) and muscle (602 and 841).

The various n-3 metabolites, including $^2H_5$-20:3n-3, $^2H_5$-20:4n-3, $^2H_5$-20:5n-3, $^2H_5$-22:5n-3, and $^2H_5$-22:6n-3, showed somewhat different accumulation in rat tissues (Table 2). The area under the curves for the intermediate $^2H_5$-20:3n-3 accumulated mainly in white adipose tissue (21.9), followed by muscle (11.5) and skin (7.8). $^2H_5$-20:5n-3 appeared mainly in muscle (33.1) but also liver (22.3), white adipose tissue (16.1), and carcass (15.1). $^2H_5$-22:5n-3 accumulated in muscle (165), white adipose (92.4), carcass (78.8), and liver (55.8). Similarly, $^2H_5$-22:6n-3 accumulated mainly in muscle (680), liver (416), carcass (274), and white adipose (256).

For the n-6 metabolites $^2H_5$-18:3n-6, $^2H_5$-20:3n-6, $^2H_5$-20:4n-6, $^2H_5$-22:4n-6, and $^2H_5$-22:5n-6, the tissue accumulation exhibited localization to particular tissues (Table 2). The intermediate $^2H_5$-18:3n-6 accumulated mainly in liver but at a low level (4.4). $^2H_5$-20:3n-6 appeared in muscle (27.3), white adipose tissue (16.6), and carcass (13.3), followed by liver (8.5). $^2H_5$-20:4n-6 (773) was among the most highly accumulated metabolite in the body; mainly occurring in muscle (210), liver (153), carcass (115), skin (108), and white adipose tissue (45.7). A tissue accumulation similar to that of $^2H_5$-20:4n-6 was observed for $^2H_5$-22:4n-6. The n-6 end product $^2H_5$-22:5n-6 exhibited the unique attribute of a very high accumulation in testis (16.6), followed by muscle (14.6), adipose (9.8), and liver (6.0).

DISCUSSION

Fate of n-3 and n-6 precursors

To our knowledge, no previous study has attempted to follow the uptake and metabolism of the EFAs 18:2n-6 and

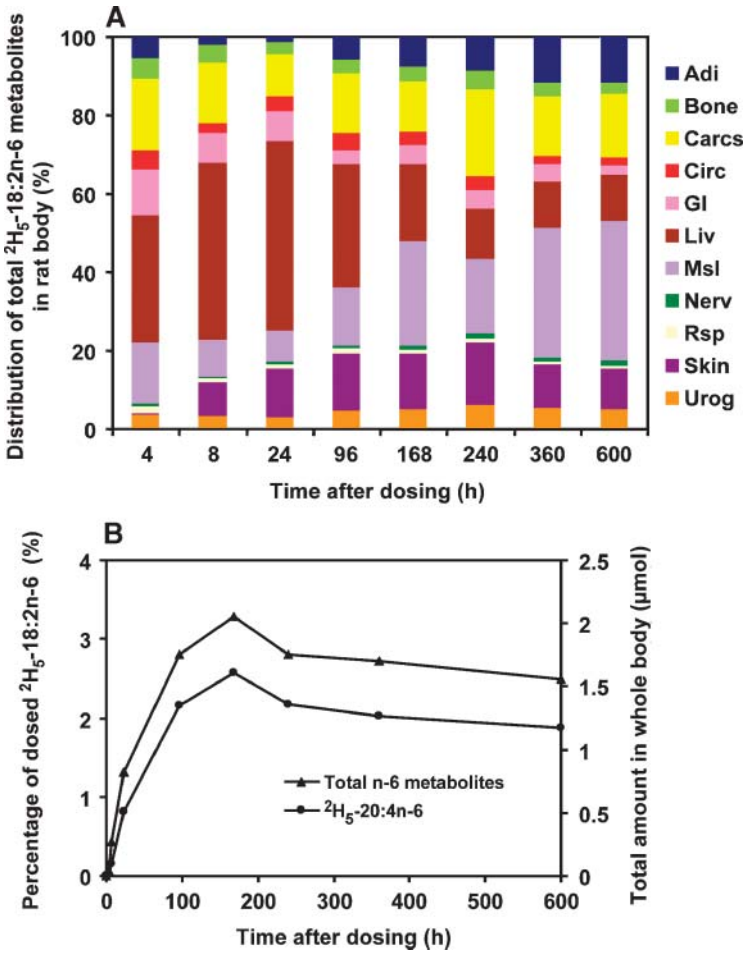

Fig. 7. Distribution of n-6 metabolites, including $^2H_5$-18:3n-6, $^2H_5$-20:3n-6, $^2H_5$-20:4n-6, $^2H_5$-22:4n-6, and $^2H_5$-22:5n-6, synthesized from $^2H_5$-18:2n-6 in rat organ systems versus time. The data are expressed as the percentage of the total recovered n-6 deuterated metabolites at each time point in A. The total amount of n-6 metabolites and $^2H_5$-20:4n-6 derived from $^2H_5$-18:2n-6 and the percentage of the initial $^2H_5$-18:2n-6 dose are presented in B. Values were derived from one animal at each time point. The abbreviations for each organ system are as in Fig. 1.

18:3n-3 throughout all of the various tissues in a mammal. This study systematically followed both the time course and the individual tissue accumulations of a pulse of deuterated C18 EFA precursors along with their principal metabolites in rats consuming a controlled and well-defined diet. Because of the magnitude of this study design, it was necessary to fix some variables, such as the diet composition and the animal age, rather than to study variations in these parameters. It must be conceded that somewhat different results may have been obtained had the macronutrients or EFA content of the diet been altered or had younger or older animals been studied. These are important variables for future study. The pulse of isotope gives a rapid early enrichment that becomes progressively diluted with subsequent dietary EFA, with the result that subsequent metabolism has less isotope per molecule metabolized.

In the past, many researchers have emphasized differences in metabolism for 18:2n-6 and 18:3n-3. One common observation has been the low level of 18:3n-3 in tissue complex lipids, as there is often an abundance of 18:2n-6 in these pools (19). It is instructive then to compare the disposition of each EFA precursor in terms of the tissue disposition, anabolic metabolism, and catabolism/excretion and to compare the n-3 and n-6 families in these respects. The net accumulation of the two labels in tissue pools was very similar, with both approaching 20% of the original dosage (compare Figs. 3B and 6B). Most of this disposition occurred within the first 100 h after dosing, with little subsequent change in the ensuing 500 h. This time course coincides with the uptake of the C18 EFA precursors into adipose tissue, which is nearly complete by 100 h after dosing. It is likely then that exposure to oxidative catabolism occurs during the absorptive and circulatory phases but that little catabolism occurs after deposition in adipose.

An attempt to estimate the overall disposition of the two EFA precursors was made by averaging the values for all tissues at time points between 24 and 600 h (with the period before 24 h excluded). The remainder of the deuterated precursors not accounted for was assumed to have been excreted and/or catabolized, although this was not measured directly. There was a remarkable similarity for $^2H_5$-18:2n-6 and $^2H_5$-18:3n-3 in the percentage of dose deposited in the various tissues (~16–18%) and also in the amount that was catabolized (~79%) (**Fig. 8**). About twice as much of the $^2H_5$-18:3n-3 (6%) was accumulated as its longer chain, more unsaturated analogs than was the $^2H_5$-18:2n-6 (2.6%) during the course of this 600 h experiment. This result might not be predicted from information emphasizing that the n-3 acid is "rapidly lost" from the body. The high extent of presumed catabolism for both EFA (78.2% and 78.9%) confirms previous studies by Cunnane (20), who observed that 75–85% of C18 PUFAs

TABLE 2. Area under the time-course curves of the total amount of deuterated PUFAs in rat tissues

No.	Tissues	$^2H_5$-18:3n-3	$^2H_5$-18:3n-3 *in vivo* metabolites					$^2H_5$-18:2n-6	$^2H_5$-18:2n-6 *in vivo* metabolites				
			20:3n-3	20:4n-3	20:5n-3	22:5n-3	22:6n-3		18:3n-6	20:3n-6	20:4n-6	22:4n-6	22:5n-6
1	Adipose, brown	63	0.5	0.9	0.8	2.5	6.3	78	ND	0.4	1.5	0.4	0.6
2	Adipose, white	**5082**	**21.9**	ND	16.1	92.4	256	**5436**	ND	16.6	45.7	22.7	9.8
3	Adrenal gland	0.4	0.02	0.02	0.09	0.5	0.66	0.6	0.02	0.1	1.6	0.4	0.03
4	Bladder	0.4	0.01	0.01	0.11	0.3	0.41	0.5	0.01	0.1	0.8	0.1	0.01
5	Bone	23	0.7	0.2	3.2	17.6	55.6	34	0.1	2.7	27.3	5.5	1.2
6	Brain	Tr	ND	ND	0.08	0.8	30.5	1.0	ND	0.6	5.9	2.2	0.2
7	Carcass	116	2.7	**2.0**	15.1	78.8	274	133	0.7	13.3	115	19.0	6.0
8	Eye	0.9	0.04	0.01	0.04	0.4	2.4	1.4	ND	0.01	1.0	0.2	0.04
9	Fur	2.0	0.03	ND	0.12	0.4	0.90	5.0	0.03	0.1	0.9	0.2	ND
10	Heart	1.3	0.04	0.02	0.4	3.3	18.7	9.1	0.03	0.4	8.6	0.5	0.5
11	Intestine	14	0.4	0.4	2.2	6.5	16.3	24	0.1	2.6	22.7	4.8	0.3
12	Kidney	2.0	0.17	0.26	1.94	2.5	13.9	8.8	0.03	1.2	21.2	0.8	0.2
13	Liver	82	2.0	Tr	22.3	55.8	416	116	**4.4**	8.5	153	5.9	6.0
14	Lung	2.3	0.13	ND	1.09	3.6	5.8	7.1	0.08	0.5	8.1	1.6	0.1
15	Muscle	602	11.5	ND	**33.1**	**165**	**680**	841	ND	**29.3**	**210**	**20.5**	14.6
16	Plasma	2.7	0.03	Tr	1.2	1.6	10.6	9.3	0.12	0.3	10.1	0.2	0.2
17	Pancreas	0.1	0.02	0.02	2.7	1.1	3.3	4.3	0.12	0.4	5.2	0.2	0.1
18	Red blood cell	0.9	0.03	0.03	0.4	1.2	2.8	2.6	0.03	0.2	4.0	0.3	0.1
19	Skin	845	7.8	ND	13.3	33.8	87.2	701	ND	7.0	108	12.0	1.5
20	Salivary gland	0.3	0.03	0.07	0.5	0.5	1.2	1.8	0.03	0.6	1.7	0.1	0.04
21	Spinal cord	ND	ND	ND	0.05	0.6	7.9	0.3	ND	0.3	1.0	0.6	0.03
22	Spleen	0.3	0.06	0.02	0.3	1.6	2.4	1.2	0.01	0.2	3.5	0.7	0.1
23	Stomach	10	0.08	0.10	0.7	1.0	2.6	11	0.03	0.4	5.5	0.6	0.1
24	Thymus gland	0.5	0.1	0.02	0.1	0.4	0.6	1.7	ND	0.2	2.8	0.4	0.03
25	Testis	0.3	0.01	0.01	0.4	0.4	9.3	3.5	0.09	1.4	8.3	3.8	**16.6**
	Total	6851	48	4	116	473	1906	7431	6	87	773	104	58
	Greatest	5082	22	2	33	165	680	5436	4	29	210	23	17

Values shown are μmol*h. The trapezoid rule was applied to calculate the area under the curve from 0 to 600 h; ND indicates nondetectable; Tr, trace values (i.e., <0.005 μmol*h). Boldface numbers indicate the greatest values for the 25 components examined.

were β-oxidized and served as substrates for carbon recycling and de novo lipid synthesis (21–23). Bell, Dick, and Porter (24) also observed very active catabolism of $^2H_5$-18:3n-3 in rainbow trout. Thus, from a whole body perspective, our study indicates very similar processing for the n-3 and n-6 fatty acid precursors.

The greater accumulation of $^2H_5$-18:3n-3 metabolites relative to those of $^2H_5$-18:2n-6 should not be construed, however, to indicate greater overall metabolism of the nonlabeled pools. The plasma and liver isotopic enrichment, for example, are much greater for the $^2H_5$-18:3n-3 than for the $^2H_5$-18:2n-6, as a result of the much larger endogenous pools of unlabeled 18:2n-6 relative to those of 18:3n-3. At the 4 h time point, the enrichment of liver and plasma $^2H_5$-18:3n-3 was >14- and 8-fold, respectively, that of $^2H_5$-18:2n-6. Thus, an equivalent rate of anabolic metabolism in micromoles per unit of time at early "pulse" time points would lead to a much greater number of deuterated metabolite molecules for the n-3 pathway. The multiple pools of various metabolites in various tissues make it difficult to have precise calculations of rate. The 2-fold greater accumulation of $^2H_5$-18:3n-3 metabolites relative to those of $^2H_5$-18:2n-6 is in fact less than the difference in enrichments, and it is likely correct to say that there was

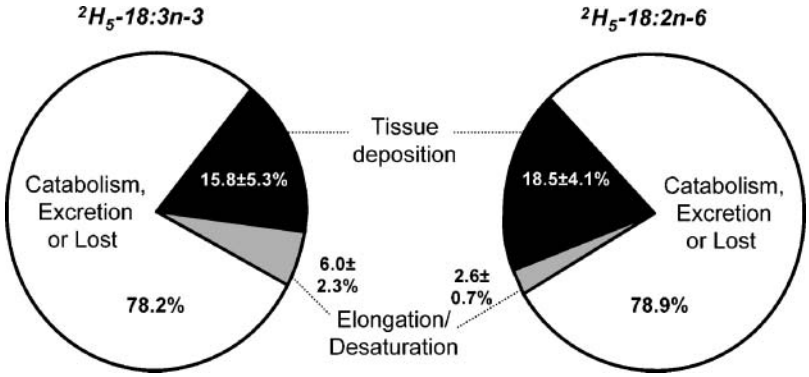

Fig. 8. Diagram of the proportions of the $^2H_5$-18:3n-3 (left panel) and $^2H_5$-18:2n-6 (right panel) dosages recovered from the rat whole body attributed to tissue deposition, elongation/desaturation, or β-oxidization, carbon recycling, excretion, and other avenues of loss from the body. Values are averaged from 1 to 25 days after the administration of precursors (mean ± SD; n = 6).

still more overall metabolism occurring in the n-6 pathway. The distribution of isotope label given as a single dose in this pulse-chase type of study is a good indicator of the fate of a dietary bolus of 18:2n-6 and 18:3n-3.

Tissue distribution of precursors

When accretion of the two precursors was compared in various tissues, the maximal amount of $^{2}H_5$-18:2n-6 was somewhat higher than that of $^{2}H_5$-18:3n-3 in most compartments, with the exceptions of skin and fur. This was in spite of a higher maximal enrichment of $^{2}H_5$-18:3n-3 in most tissues, including plasma and liver (data not shown). Both $^{2}H_5$-18:2n-6 and $^{2}H_5$-18:3n-3 reached high concentrations in the stomach and plasma at the earliest time points, consistent with their digestive and circulatory functions. There was a somewhat extended time course for 18:2n-6 with respect to that of 18:3n-3, reflecting a somewhat slower disappearance, particularly in the heart but that was also observed, to a lesser extent, in the testis, kidney, and spleen. There was then a rapid disappearance of labeled precursors by 100 h after dosing in most tissues, with most of the $^{2}H_5$-18:3n-3 and $^{2}H_5$-18:2n-6 appearing in white adipose tissue, likely reflecting accretion in triacylglycerols, the predominant form of lipids in these cells (25, 26). A fast oxidation rate for ^{14}C-18:3n-3 similar to that of lauric acid was observed by Leyton, Drury, and Crawford (9). Similarly, Cunnane and Anderson (8) found that the fate of both dietary 18:2n-6 and 18:3n-3 is largely β-oxidization. Of the remaining labeled fatty acid precursors, the rapid disappearance from many tissues is the result of the repeated large influx of nonlabeled fatty acids via the diet. In our controlled diet, the daily intake of 18:2n-6 and 18:3n-3 is estimated to be 225 and 45 mg, respectively. After 4 days, this unlabeled fatty acid will rapidly dilute pools of fatty acids that are not sequestered by cells.

Our results indicate that adipose is the primary depository for the C18 EFAs, followed by muscle and skin. This is in good agreement with the findings from dietary (8, 27) and radiotracer (28, 29) experiments. The white adipose tissue plays a storage role for the C18 EFA precursors, from which they may be mobilized by hormone-sensitive lipase. Thus, once an acid enters the large pool of acids in adipose triacylglycerols, it is unlikely to exit quickly. This phenomenon has been called "isotope trapping" when describing the slow exit of isotope from a relatively large pool. Fu and Sinclair observed that skin played an important role in the accumulation of $^{2}H_5$-18:3n-3 in the guinea pig (29). The present study of rats confirms that skin is an important depot for $^{2}H_5$-18:3n-3 (D_{max} = 3.8%); however, fur exhibited a low amount of $^{2}H_5$-18:3n-3 labeling (D_{max} = 0.2%) that was observable only at early times after dosing.

n-3 and n-6 metabolites

Only a limited amount of the labeled EFA precursors were elongated and desaturated during the first 100 h, as comparatively large amounts of the precursors were accumulated in various tissue triacylglycerols. Limited release of precursor from these pools combines with limited amounts of elongated/desaturated intermediates to keep overall amounts of isotopic precursors and metabolites relatively constant from 100 to 600 h. In vitro studies have suggested that Δ-6 desaturase may be rate limiting (30, 31). A comparison of the first two metabolic steps in rat liver microsomal elongation/desaturation in vitro indicates that the Δ-6 desaturase had the lowest reaction rate for both the n-6 and n-3 pathways (32, 33). This is in agreement with the results of studies reporting limited anabolic metabolism of 18:2n-6 and 18:3n-3 (1, 34). Cunnane and Anderson (8) estimated that 1.4% of 18:3n-3 and 3% of 18:2n-6 were converted to long-chain PUFAs in rats. However, Poumes-Ballihaut et al. (35) found that ~17% of 18:3n-3 was converted to long-chain PUFAs over a 5 week period beginning at weaning in pups with low n-3 fatty acid body stores. In our study, most of the n-3 metabolite in the rat body was in the form of $^{2}H_5$-22:6n-3 (Fig. 4B). Similarly, we noted that in most tissues, $^{2}H_5$-20:4n-6 was the predominant n-6 metabolite (Fig. 7B), with the exception of the testis, where $^{2}H_5$-22:5n-6 replaced $^{2}H_5$-20:4n-6 as the principal metabolite. For the n-3 pathway, the $^{2}H_5$-20:5n-3 elongation product, $^{2}H_5$-22:5n-3, was found at a higher concentration than its precursor in the tissues examined, with the exception of the testis. Upon inspection of Fig. 2, it is apparent that the $^{2}H_5$-20:5n-3 disappeared faster than the $^{2}H_5$-22:6n-3 in several tissues, including the RBCs, liver, heart, brain, spinal cord, testis, and eye. In addition to its greater metabolism, the more rapid disappearance of 20:5n-3 may be attributable to the observation that 20:5n-3 is more readily β-oxidized than 20:4n-6 or 22:6n-3 (36).

Tissue distribution of metabolites

The rat liver exhibited the highest C_{max} of the $^{2}H_5$-18:3n-3 metabolites $^{2}H_5$-20:5n-3, $^{2}H_5$-22:5n-3, and $^{2}H_5$-22:6n-3 among the main organs between 8 and 96 h after dosing. For the $^{2}H_5$-18:2n-6 metabolites, the C_{max} values were observed sequentially for $^{2}H_5$-18:3n-6, then $^{2}H_5$-20:3n-6, and finally $^{2}H_5$-20:4n-6 in the liver during the period from 8 to 168 h after dosing, following the expected pattern as prescribed by the known metabolic sequence. This was consistent with the prevailing view that the liver represents the primary site of EFA elongation/desaturation. The plasma distributions of the various labeled n-3 and n-6 metabolites were similar to the liver time course or, in some cases, a bit delayed, as would be expected if the liver metabolites were rapidly exported to the plasma. Similarly, the EFA metabolite time-course plots of some tissues (e.g., lung and spleen) were similar to that of the plasma; however, others, most notably heart, exhibited a later maximum.

In brown adipose tissue, the $^{2}H_5$-20:4n-6 and $^{2}H_5$-22:6n-3 maximal concentrations were approximately twice those in white adipose tissue; however, they both contained a similar concentration of the C18 precursors. In general, the ratio of the principal metabolite to precursor was relatively high for both the n-3 and n-6 fatty acids, approaching 1 or greater in several tissues, but was much lower in liver and plasma. One explanation for this is that in many organs the metabolites are preferentially incorporated into phospholipids, reflecting acyltransferase selec-

JOURNAL OF LIPID RESEARCH ASBMB

tivities (37, 38) rather than the precursors that eventually accumulated in adipose triacylglycerols.

Another group of tissues including the brain, spinal cord, eye, testis, and RBCs had the characteristic that the C22 PUFAs peaked after a rather long period and then remained high. Investigators made a similar observation in the baboon neonate and suggested that slow turnover of RBC 22:6n-3 correlates with the brain and retinal 22:6n-3 but that plasma correlates better with liver, which secretes lipid to plasma (39). These tissues accumulate and retain these n-3 and n-6 C22 PUFAs beyond 25 days, primarily in phospholipids. This is consistent with the well-known retention of 22:6n-3 in the nervous system, where it can support its vital functions (40). The various nervous system tissues studied here did not all respond in the same manner with respect to their content of the C18 precursors and their metabolites. The brain and spinal cord $^{2}H_5$-18:3n-3 contents were essentially nil, and only traces of $^{2}H_5$-20:5n-3 were detected. The observation of slightly greater levels of $^{2}H_5$-22:5n-3 and much higher levels of $^{2}H_5$-22:6n-3 indicates that (1) shorter chain metabolites were very rapidly metabolized to their C22 products, (2) the primary accretion mechanism for $^{2}H_5$-22:6n-3 was the uptake of preformed molecules from the circulation, or (3) 18:3n-3 and 20:5n-3 are somehow excluded from many phospholipids and are then β-oxidized. The second conclusion is consistent with other studies (26, 41–43), although it has been proposed that $^{2}H_5$-22:5n-3 may also be exported from the liver and taken up into the brain (44).

However, an appreciable amount of $^{2}H_5$-18:3n-3 was found in the eye relative to $^{2}H_5$-22:6n-3 content, although the $^{2}H_5$-20:5n-3 was again very low. Only the retina is nervous system tissue, and the results may have been different if only this subcomponent had been analyzed. Similarly, the $^{2}H_5$-18:2n-6 content in eye was even higher than that of its C20 and C22 metabolites, and this allows for the possibility of local metabolism. The availability of the C18 precursors in the eye makes possible the local biosynthesis of 22:6n-3 or 20:4n-6 (45, 46), which may then be supplied to the retina. Similarly, the metabolism of ^{14}C-18:3n-3 to 22:6n-3 has been observed after injection into the brain (47, 48). The n-6 precursor was also taken up into the brain and spinal cord to a much greater extent than the n-3 precursor, and it was of a similar order of magnitude as its metabolites. Such preferential accretion of 18:2n-6 has been observed previously in the mouse brain (19). However, although the nervous system accumulated and retained $^{2}H_5$-22:6n-3 and $^{2}H_5$-20:4n-6 beyond 25 days, the maximal amount detected in brain only accounted for 0.1% and 0.02% of the respective C18 precursor doses. This degree of labeling was similar to that observed previously for suckling rats (19), the labeling of fetal rhesus brain after dosing the mother with ^{13}C-U-18:3n-3 (0.24%) (34), and when ^{14}C-18:3n-3 (49) or ^{14}C-18:2n-6 (50) was infused intravenously in adult rats. However, a much greater uptake into mammalian brain was obtained when the animals were dosed with preformed 22:6n-3 and 20:4n-6 in the range of ~2–4.5% of the dosages (26, 34, 51). In one experiment, intravenously injected ^{11}C-20:4n-6 led to brain radioactivity accounting for 7% of the injected amount (52). Thus, it is apparent that preformed 22:6n-3 and 20:4n-6 are much better sources of brain 22:6n-3 and 20:4n-6 than their C18 precursors and that precursor metabolism is a minor source of these brain PUFAs.

For the principal n-3 ($^{2}H_5$-22:6n-3) and n-6 ($^{2}H_5$-20:4n-6) metabolites, the organs in which the greatest amounts accumulated overall were the liver, muscle, skin, and adipose. In muscle, in particular, it was quite possible that local metabolism of the EFA precursors had occurred. In this regard, it was also noteworthy that the concentrations of $^{2}H_5$-22:4n-6 (2-fold) and $^{2}H_5$-22:5n-6 (6-fold) were greater in testis than those in liver. Although it is possible that the testis concentrates these fatty acids against a concentration gradient, another possible interpretation of these data is that there is local elongation/desaturation of the n-6 fatty acids in testis.

One potential application of this multicompartmental analysis concerns the issue of understanding to what extent analyses of blood in human studies may reflect the stable isotope metabolism of internal organs that cannot be sampled. A long-standing issue has been, for example, how well do plasma stable isotope metabolites reflect activity in the liver or brain from both a qualitative and a quantitative standpoint? As noted above, there is little correlation between these compartments with respect to C18 content; however, C20 and C22 PUFAs in the brain have a pattern that is more similar to that of the RBCs than the plasma. The RBC 22:6n-3 level, in particular, may be somewhat reflective of that of the nervous system, as has been suggested previously in studies of the baboon (39). The plasma lipids secreted by liver provide a reasonable reflection of rat liver metabolism, although C22 PUFAs appear to have a somewhat greater labeling in the liver. Thus, blood analyses do provide some insight into the metabolic processes of other key organs in the rat and in nonhuman primates, and it is reasonable then to expect a similar situation in humans.

The authors acknowledge Dr. William E. M. Lands for valuable suggestions on the manuscript and encouragement on this project. Thanks also to Dr. Lee Chedester and Mr. Marshall Jones for their valuable advice and expert assistance with the animal work. This project was funded by the Intramural Research Program of the National Institute on Alcohol Abuse and Alcoholism, National Institutes of Health.

REFERENCES

1. Pawlosky, R. J., J. R. Hibbeln, J. A. Novotny, and N. Salem, Jr. 2001. Physiological compartmental analysis of alpha-linolenic acid metabolism in adult humans. *J. Lipid Res.* **42:** 1257–1265.
2. Pawlosky, R. J., J. R. Hibbeln, Y. H. Lin, S. Goodson, P. Riggs, N. Sebring, G. L. Brown, and N. Salem, Jr. 2003. Effects of beef- and fish-based diets on the kinetics of n-3 fatty acid metabolism in human subjects. *Am. J. Clin. Nutr.* **77**: 565–572.
3. Goyens, P. L., M. E. Spilker, P. L. Zock, M. B. Katan, and R. P. Mensink. 2005. Compartmental modeling to quantify alpha-linolenic acid conversion after longer term intake of multiple tracer boluses. *J. Lipid Res.* **46:** 1474–1483.

4. Sheaff, R. C., H. M. Su, L. A. Keswick, and J. T. Brenna. 1995. Conversion of alpha-linolenate to docosahexaenoate is not depressed by high dietary levels of linoleate in young rats: tracer evidence using high precision mass spectrometry. *J. Lipid Res.* **36:** 998–1008.
5. Su, H. M., T. N. Corso, P. W. Nathanielsz, and J. T. Brenna. 1999. Linoleic acid kinetics and conversion to arachidonic acid in the pregnant and fetal baboon. *J. Lipid Res.* **40:** 1304–1312.
6. Fu, Z., N. M. Attar-Bashi, and A. J. Sinclair. 2001. 1-^{14}C-linoleic acid distribution in various tissue lipids of guinea pigs following an oral dose. *Lipids.* **36:** 255–260.
7. Fu, Z., and A. J. Sinclair. 2000. Increased alpha-linolenic acid intake increases tissue alpha-linolenic acid content and apparent oxidation with little effect on tissue docosahexaenoic acid in the guinea pig. *Lipids.* **35:** 395–400.
8. Cunnane, S. C., and M. J. Anderson. 1997. The majority of dietary linoleate in growing rats is beta-oxidized or stored in visceral fat. *J. Nutr.* **127:** 146–152.
9. Leyton, J., P. J. Drury, and M. A. Crawford. 1987. Differential oxidation of saturated and unsaturated fatty acids in vivo in the rat. *Br. J. Nutr.* **57:** 383–393.
10. Reeves, P. G., F. H. Nielsen, and G. C. Fahey, Jr. 1993. AIN-93 purified diets for laboratory rodents: final report of the American Institute of Nutrition ad hoc writing committee on the reformulation of the AIN-76A rodent diet. *J. Nutr.* **123:** 1939–1951.
11. Moriguchi, T., S. Y. Lim, R. Greiner, W. Lefkowitz, J. Loewke, J. Hoshiba, and N. Salem, Jr. 2004. Effects of an n-3-deficient diet on brain, retina, and liver fatty acyl composition in artificially reared rats. *J. Lipid Res.* **45:** 1437–1445.
12. Watkins, B. A., C. L. Shen, J. P. McMurtry, H. Xu, S. D. Bain, K. G. Allen, and M. F. Seifert. 1997. Dietary lipids modulate bone prostaglandin E2 production, insulin-like growth factor-I concentration and formation rate in chicks. *J. Nutr.* **127:** 1084–1091.
13. Folch, A. C., M. Lees, and G. M. Sloane-Stanley. 1957. A simple method for isolation and purification of total lipids from animal tissues. *J. Biol. Chem.* **226:** 497–509.
14. Morrison, W. R., and L. M. Smith. 1964. Preparation of fatty acid methyl esters and dimethyl acetals from lipids with boron tri-fluoride-methanol. *J. Lipid Res.* **5:** 600–608.
15. Salem, N., Jr., M. Reyzer, and J. Karanian. 1996. Losses of arachidonic acid in rat liver after alcohol inhalation. *Lipids.* **31 (Suppl.):** 153–156.
16. Pawlosky, R. J., H. W. Sprecher, and N. Salem, Jr. 1992. High sensitivity negative ion GC-MS method for detection of desaturated and chain-elongated products of deuterated linoleic and linolenic acids. *J. Lipid Res.* **33:** 1711–1717.
17. Lin, Y. H., and N. Salem, Jr. 2005. In vivo conversion of 18- and 20-C essential fatty acids in rats using the multiple simultaneous stable isotope method. *J. Lipid Res.* **46:** 1962–1973.
18. Yeh, K. C., and K. C. Kwan. 1978. A comparison of numerical integrating algorithms by trapezoidal, Lagrange, and spline approximation. *J. Pharmacokinet. Biopharm.* **6:** 79–98.
19. Pawlosky, R. J., G. Ward, and N. Salem, Jr. 1996. Essential fatty acid uptake and metabolism in the developing rodent brain. *Lipids.* **31 (Suppl.):** 103–107.
20. Cunnane, S. C. 1996. The Canadian Society for Nutritional Sciences 1995 Young Scientist Award Lecture. Recent studies on the synthesis, beta-oxidation, and deficiency of linoleate and alpha-linolenate: are essential fatty acids more aptly named indispensable or conditionally dispensable fatty acids? *Can. J. Physiol. Pharmacol.* **74:** 629–639.
21. Menard, C. R., K. J. Goodman, T. N. Corso, J. T. Brenna, and S. C. Cunnane. 1998. Recycling of carbon into lipids synthesized de novo is a quantitatively important pathway of alpha-[U-^{13}C] linolenate utilization in the developing rat brain. *J. Neurochem.* **71:** 2151–2158.
22. Cunnane, S. C., M. A. Ryan, C. R. Nadeau, R. P. Bazinet, K. Musa-Veloso, and U. McCloy. 2003. Why is carbon from some polyunsaturates extensively recycled into lipid synthesis? *Lipids.* **38:** 477–484.
23. Cunnane, S. C., M. A. Ryan, Y. H. Lin, S. Y. Lim, and N. Salem, Jr. 2006. Suckling rats actively recycle carbon from {alpha}-linolenate into newly synthesized lipids even during extreme dietary deficiency of n-3 polyunsaturates. *Pediatr. Res.* **59:** 107–110.
24. Bell, M. V., J. R. Dick, and A. E. Porter. 2003. Pyloric ceca are significant sites of newly synthesized 22:6n-3 in rainbow trout (*Oncorhynchus mykiss*). *Lipids.* **38:** 39–44.
25. Bates, M. W. 1958. Turnover rates of fatty acids of plasma triglyceride, cholesterol ester and phospholipid in the postabsorptive dog. *Am. J. Physiol.* **194:** 446–452.
26. Sinclair, A. J. 1975. Incorporation of radioactive polyunsaturated fatty acids into liver and brain of developing rat. *Lipids.* **10:** 175–184.
27. Bourre, J. M., M. Piciotti, O. Dumont, G. Pascal, and G. Durand. 1990. Dietary linoleic acid and polyunsaturated fatty acids in rat brain and other organs. Minimal requirements of linoleic acid. *Lipids.* **25:** 465–472.
28. Leyton, J., P. J. Drury, and M. A. Crawford. 1987. In vivo incorporation of labeled fatty acids in rat liver lipids after oral administration. *Lipids.* **22:** 553–558.
29. Fu, Z., and A. J. Sinclair. 2000. Novel pathway of metabolism of alpha-linolenic acid in the guinea pig. *Pediatr. Res.* **47:** 414–417.
30. Mead, J. F. 1958. The metabolism of the essential fatty acids. *Am. J. Clin. Nutr.* **6:** 656–661.
31. Hassam, A. G., A. J. Sinclair, and M. A. Crawford. 1975. The incorporation of orally fed radioactive gamma-linolenic acid and linoleic acid into the liver and brain lipids of suckling rats. *Lipids.* **10:** 417–420.
32. Marcel, Y. L., K. Christiansen, and R. T. Holman. 1968. The preferred metabolic pathway from linoleic acid to arachidonic acid in vitro. *Biochim. Biophys. Acta.* **164:** 25–34.
33. Sprecher, H. 1986. Comparison of omega-3 and omega-6 fatty acid metabolism. *In* Health Effects of Polyunsaturated Fatty Acids in Seafoods. A. P. Simopoulos, R. R. Kifer, and R. E. Martin, editors. Academic Press, New York. 353–379.
34. Sheaff Greiner, R. C., Q. Zhang, K. J. Goodman, D. A. Giussani, P. W. Nathanielsz, and J. T. Brenna. 1996. Linoleate, alpha-linolenate, and docosahexaenoate recycling into saturated and monounsaturated fatty acids is a major pathway in pregnant or lactating adults and fetal or infant rhesus monkeys. *J. Lipid Res.* **37:** 2675–2686.
35. Poumes-Ballihaut, C., B. Langelier, F. Houlier, J. M. Alessandri, G. Durand, C. Latge, and P. Guesnet. 2001. Comparative bioavailability of dietary alpha-linolenic and docosahexaenoic acids in the growing rat. *Lipids.* **36:** 793–800.
36. Gavino, G. R., and V. C. Gavino. 1991. Rat liver outer mitochondrial carnitine palmitoyltransferase activity towards long-chain polyunsaturated fatty acids and their CoA esters. *Lipids.* **26:** 266–270.
37. Holub, B. J. 1984. 1982 Borden Award Lecture. Nutritional, biochemical, and clinical aspects of inositol and phosphatidylinositol metabolism. *Can. J. Physiol. Pharmacol.* **62:** 1–8.
38. Lands, W. E., M. Inoue, Y. Sugiura, and H. Okuyama. 1982. Selective incorporation of polyunsaturated fatty acids into phosphatidylcholine by rat liver microsomes. *J. Biol. Chem.* **257:** 14968–14972.
39. Sarkadi-Nagy, E., V. Wijendran, G. Y. Diau, A. C. Chao, A. T. Hsieh, A. Turpeinen, P. Lawrence, P. W. Nathanielsz, and J. T. Brenna. 2004. Formula feeding potentiates docosahexaenoic and arachidonic acid biosynthesis in term and preterm baboon neonates. *J. Lipid Res.* **45:** 71–80.
40. Salem, N., Jr. 1989. Omega-3 fatty acids: molecular and biochemical aspects. *In* Current Topics in Nutrition and Disease: New Protective Roles for Selected Nutrients. G. A. Spiller and J. Scala, editors. Alan R. Liss, New York. 109–228.
41. Abedin, L., E. L. Lien, A. J. Vingrys, and A. J. Sinclair. 1999. The effects of dietary alpha-linolenic acid compared with docosahexaenoic acid on brain, retina, liver, and heart in the guinea pig. *Lipids.* **34:** 475–482.
42. Bowen, R. A., and M. T. Clandinin. 2000. High dietary 18:3n-3 increases the 18:3n-3 but not the 22:6n-3 content in the whole body, brain, skin, epididymal fat pads, and muscles of suckling rat pups. *Lipids.* **35:** 389–394.
43. Lefkowitz, W., S. Y. Lim, Y. H. Lin, and N. Salem. 2005. Where does the developing brain obtain its docosahexaenoic acid? Relative contributions of dietary alpha-linolenic acid, docosahexaenoic acid, and body stores in the developing rat. *Pediatr. Res.* **57:** 157–165.
44. Pawlosky, R., A. Barnes, and N. Salem, Jr. 1994. Essential fatty acid metabolism in the feline: relationship between liver and brain production of long-chain polyunsaturated fatty acids. *J. Lipid Res.* **35:** 2032–2040.
45. Bell, M. V., J. R. Dick, and A. E. Porter. 2003. Tissue deposition of n-3 FA pathway intermediates in the synthesis of DHA in rainbow trout (*Oncorhynchus mykiss*). *Lipids.* **38:** 925–931.
46. Bazan, H. E., M. M. Careaga, H. Sprecher, and N. G. Bazan. 1982. Chain elongation and desaturation of eicosapentaenoate to docosahexaenoate and phospholipid labeling in the rat retina in vivo. *Biochim. Biophys. Acta.* **712:** 123–128.

47. Dhopeshwarkar, G. A., and C. Subramanian. 1976. Biosynthesis of polyunsaturated fatty acids in the developing brain. I. Metabolic transformations of intracranially administered 1-^{14}C linolenic acid. *Lipids.* **11:** 67–71.
48. Dwyer, B. E., and J. Bernsohn. 1979. The effect of essential fatty acid deprivation on the metabolic transformations of [1(-14)C] linolenate in developing rat brain. *Biochim. Biophys. Acta.* **575:** 309–317.
49. DeMar, J. C., Jr., K. Ma, L. Chang, J. M. Bell, and S. I. Rapoport. 2005. α-Linolenic acid does not contribute appreciably to docosahexaenoic acid within brain phospholipids of adult rats fed a diet enriched in docosahexaenoic acid. *J. Neurochem.* **94:** 1063–1076.
50. DeMar, J. C., Jr., H. J. Lee, K. Ma, L. Chang, J. M. Bell, S. I. Rapoport, and R. P. Bazinet. 2006. Brain elongation of linoleic acid is a negligible source of the arachidonate in brain phospholipids of adult rats. *Biochim. Biophys. Acta.* **1761:** 1050–1059.
51. Wijendran, V., M. C. Huang, G. Y. Diau, G. Boehm, P. W. Nathanielsz, and J. T. Brenna. 2002. Efficacy of dietary arachidonic acid provided as triglyceride or phospholipid as substrates for brain arachidonic acid accretion in baboon neonates. *Pediatr. Res.* **51:** 265–272.
52. Chang, M. C., T. Arai, L. M. Freed, S. Wakabayashi, M. A. Channing, B. B. Dunn, M. G. Der, J. M. Bell, T. Sasaki, P. Herscovitch, et al. 1997. Brain incorporation of [1-^{11}C]arachidonate in normocapnic and hypercapnic monkeys, measured with positron emission tomography. *Brain Res.* **755:** 74–83.